Spin-wave spectra of insulating films: Comparison of exact calculations and a single-wave-vector model

Andrzej Maksymowicz
Department of Solid State Physics, Academy of Mining and Metallurgy, PL-30-059 Kraków, Aleje Mickiewicza 30, Poland
(Received 26 December 1984; revised manuscript received 20 September 1985)

Spin-wave spectra are usually calculated within the circular-precession approximation which neglects ellipticity of the microwave magnetization. This approximation yields rigorously correct results only for perpendicular resonance and becomes worse for parallel resonance. Even if the ellipticity is accounted for, only single-wave-vector modes are commonly postulated for nonperpendicular resonance. Such modes cannot satisfy the boundary conditions except for zero surface anisotropy energy when the model is exact for any configuration of applied external field. Rigorous results correspond to normal modes made up of waves with two different wave vectors. Calculations with a set of parameters typical for a 1000-Å-thick Permalloy film indicate that the exact results may significantly differ from the single-wave-vector model both in the position of the normal modes and their intensities. The predicted critical angle is also different from the $\pi/4$ observed. It is concluded that the exact procedure is, in principle, required.

I. INTRODUCTION

The quality of a spin-wave-resonance spectrum depends on the quality of the sample. The main factors affecting it are the homogeneity of the film and conditions on the two surfaces. Volume inhomogeneity (VI) models[1-3] must be employed when the saturation magnetization M varies in the bulk of the film. In this paper we assume a uniform $\mathbf{M}$ so that the surface inhomogeneity (SI) model[4-7] is applicable. Calculations of the spectra, the resonance field H_n, and the intensity I_n of the nth mode, are based on the surface pinning parameters introduced by the boundary conditions.

A circular precession of the dynamic magnetization takes place for perpendicular resonance when a magnetic field is applied along the normal of the film plane. The wave vector k is a good quantum number and the boundary conditions yield allowed k_n from which H_n and I_n of the nth mode are obtained. The precession is elliptical if the magnetic field is out of the perpendicular configuration. However, the circular-precession approximation may still be applied,[4-6] provided the deviation from the circular precession is not too large. Better approaches[6-10] account for ellipticity. However, in most cases a solution for the dynamic microwave magnetization is assumed to be a single-wave-vector mode (SWM) characterized by one k only. A normal mode is actually made up of two waves with different wave vectors,[6,11,12] but one of the waves is claimed to be negligible since the corresponding wave vector is always imaginary and usually large. However, both waves must be accounted for if the boundary conditions for the microwave components on both surfaces are to be satisfied. It may then be desirable to compare the SWM model and the exact calculations presented in this paper to see whether the two procedures agree.

The equation of motion for spins inside the film and on the surfaces is discussed in Sec. II. The numerical procedure for any set of pinning conditions is summarized in Sec. III. The model is applied to the case of uniaxial surface anisotropy and uniaxial bulk magnetic energy in Sec. IV. Results of calculations for a thin Permalloy film and comparison of the SWM model with the model presented here are given in Sec. V, followed by a discussion in Sec. VI.

Recently, a similar model based on two wave vectors was independently worked out and presented in a series of papers[13-15] for symmetrical or antisymmetrical pinning conditions.

II. MODEL

The equation of motion for the magnetization is given by

$$\frac{1}{\gamma}\frac{d(\mathbf{M}+\mathbf{m})}{dt}=(\mathbf{M}+\mathbf{m})\times(\mathbf{H}_i+\mathbf{h}_i)+(\mathbf{M}+\mathbf{m})\times\mathbf{H}_e+\mathbf{T}-\mathbf{S}\ , \tag{1}$$

where the magnetization $\mathbf{M}+\mathbf{m}$ is the sum of static $\mathbf{M}$ and dynamic $\mathbf{m}$ components. Static $\mathbf{H}_i$ and dynamic $\mathbf{h}_i$ internal magnetic fields are subject to Maxwell's equations. The exchange field in the bulk

$$H_e=\frac{2A}{M^2}\nabla^2(\mathbf{M}+\mathbf{m}) \tag{2}$$

is different from the value at the surface of the film,

$$H_e=\frac{2A}{M^2}\left[\frac{1}{a}\partial_n(\mathbf{M}+\mathbf{m})\right], \tag{3}$$

where A is the exchange constant, a is the lattice parameter, and ∂_n is the normal outward derivative. The torque $\mathbf{T}$ comprises all other magnetic energies E,

$$\mathbf{T}=\hat{\boldsymbol{\vartheta}}\frac{1}{\sin\vartheta}\frac{\partial E}{\partial\varphi}-\hat{\boldsymbol{\varphi}}\frac{\partial E}{\partial\vartheta}\ , \tag{4}$$

where $\hat{\vartheta}$ and $\hat{\varphi}$ are unit vectors in the ϑ and φ directions, respectively, in the spherical coordinate system. The damping term **S** will be ignored since we are interested in normal modes.

The static magnetization **M** is assumed to be uniform in the bulk of the film situated in the x-y plane. For the external magnetic field H applied in the θ,ϕ directions one obtains the equilibrium condition from the static part of Eq. (1):

$$\frac{\partial \tilde{E}}{\partial \vartheta}=0, \quad \frac{\partial \tilde{E}}{\partial \varphi}=0 , \tag{5}$$

where

$$\tilde{E}(\varphi,\vartheta)=E(\varphi,\vartheta)-\mathbf{M}\cdot\mathbf{H}-2\pi M^2\sin^2\vartheta . \tag{6}$$

The dynamic part of Eq. (1) yields, for $\mathbf{m}=m_\vartheta\hat{\vartheta}+m_\varphi\hat{\varphi}$ in the film,

$$\begin{aligned} &\frac{1}{4\pi M\gamma}\frac{dm_\vartheta}{dt}-Rm_\vartheta-Pm_\varphi+d\nabla^2 m_\varphi=0 , \\ &\frac{1}{4\pi M\gamma}\frac{dm_\varphi}{dt}+Rm_\varphi+Qm_\vartheta-d\nabla^2 m_\vartheta=0 , \end{aligned} \tag{7}$$

where

$$\begin{aligned} P&=\frac{1}{4\pi M^2}\frac{1}{\sin^2\vartheta}\frac{\partial^2\tilde{E}}{\partial\varphi^2} , \\ Q&=\frac{1}{4\pi M^2}\frac{\partial^2\tilde{E}}{\partial\vartheta^2} , \\ R&=\frac{1}{4\pi M^2}\frac{1}{\sin\vartheta}\frac{\partial^2\tilde{E}}{\partial\varphi\partial\vartheta} \end{aligned} \tag{8}$$

are taken at the equilibrium values ϑ,φ given by Eq. (5) and the stiffness constant is

$$d=\frac{2A}{4\pi M^2} . \tag{9}$$

For a wavelike form of $m\sim\exp[i(\omega t-kz)]$ one obtains the dispersion relation

$$\Omega^2=(P+k^2d)(Q+k^2d)-R^2 , \tag{10}$$

where

$$\Omega=\frac{\omega}{4\pi M\gamma} . \tag{11}$$

From Eq. (10) we have

$$k^2d=\left[\left[\frac{P-Q}{2}\right]^2+R^2+\Omega^2\right]^{1/2}-\frac{P+Q}{2} , \tag{12}$$

and for $k^2d>0$ the microwave component is of a sinusoidal form describing volume modes. For $k^2d<0$, when $k=i\mu$, we obtain surface modes. The other solution of Eq. (10) provides only imaginary wave vectors $k=i\tau$,

$$\tau^2d=\left[\left[\frac{P-Q}{2}\right]^2+R^2+\Omega^2\right]^{1/2}+\frac{P+Q}{2} . \tag{13}$$

Let us consider a film of thickness L, $-L/2\le z\le L/2$. The general solution is a superposition of the k (or μ) and τ modes:

$$\begin{aligned} m_\vartheta&=\alpha e^+g^-\sin(kz)+\beta e^+g^-\cos(kz)+\gamma e^-g^-\exp(-\tau L/2)\sinh(\tau z)+\delta e^-g^-\exp(-\tau L/2)\cosh(\tau z) , \\ m_\varphi/i&=\alpha e^-g^+\sin(kz)+\beta e^-g^+\cos(kz)-\gamma e^+g^+\exp(-\tau L/2)\sinh(\tau z)-\delta e^+g^+\exp(-\tau L/2)\cosh(\tau z) \end{aligned} \tag{14}$$

for the volume modes and

$$\begin{aligned} m_\vartheta&=\alpha e^+g^-\exp(-\mu L/2)\sinh(\mu z)+\beta e^+g^-\exp(-\mu L/2)\cosh(\mu z)+\gamma e^-g^-\exp(-\tau L/2)\sinh(\tau z) \\ &\quad+\delta e^-g^-\exp(-\tau L/2)\cosh(\tau z) , \\ m_\varphi/i&=\alpha e^-g^+\exp(-\mu L/2)\sinh(\mu z)+\beta e^-g^+\exp(-\mu L/2)\cosh(\mu z)-\gamma e^+g^+\exp(-\tau L/2)\sinh(\tau z) \\ &\quad-\delta e^+g^+\exp(-\tau L/2)\cosh(\tau z) \end{aligned} \tag{15}$$

for the surface modes, where α, β, γ, and δ are constants to be found later on. The $\exp(\cdots)$ factors were excluded from the constants only for numerical reasons, to prevent us from having to deal with large numbers. Other symbols used in Eqs. (14) and (15) are

$$e^\pm=[(\Omega^2+R^2+\Delta^2)^{1/2}\pm\Delta]^{1/2}, \quad \Delta=(P-Q)/2 \tag{16}$$

$$g^\pm=1\pm iR/[\Omega+(\Omega^2+R^2)^{1/2}] . \tag{17}$$

The microwave magnetization distribution across the film thickness is given by Eqs. (14) and (15), provided the constants α, β, γ, and δ are known. The constants are obtained from the boundary conditions resulting from the equation of motion for spins on the surface. These spins experience different exchange fields, Eq. (3). Also, an extra torque can be due to the surface energy per unit area, $F(\varphi,\vartheta)$. Therefore the equation of motion for the surface spins is different from the bulk equation. From the static part of the equation we obtain

$$\begin{aligned} &\frac{2A}{M}(\partial_n\mathbf{M})_\varphi+\frac{1}{\sin\vartheta}\frac{\partial F}{\partial\varphi}=0 , \\ &\frac{2A}{M}(\partial_n\mathbf{M})_\vartheta+\frac{\partial F}{\partial\vartheta}=0 , \end{aligned} \tag{18}$$

for the $\hat{\varphi}$ and $\hat{\vartheta}$ components of the normal derivative $\partial_n \mathbf{M}$. The dynamic part, after employing Eq. (18), provides boundary conditions[6,16,17] of the form

$$\begin{aligned} &\partial_n m_\vartheta + p m_\vartheta + r m_\varphi = 0 , \\ &\partial_n m_\varphi + q m_\varphi + r m_\vartheta = 0 , \end{aligned} \tag{19}$$

where

$$\begin{aligned} p &= \frac{1}{2A}\frac{\partial^2 F}{\partial \vartheta^2} - (\partial_n M)/M , \\ q &= \frac{1}{2A}\left[\frac{\cos\vartheta}{\sin\vartheta}\frac{\partial F}{\partial \vartheta} + \frac{1}{\sin^2\vartheta}\frac{\partial^2 F}{\partial \varphi^2}\right] - (\partial_n M)/M , \\ r &= \frac{1}{2A}\left[-\frac{\cos\vartheta}{\sin^2\vartheta}\frac{\partial F}{\partial \varphi} + \frac{1}{\sin\vartheta}\frac{\partial^2 F}{\partial \vartheta \partial \varphi}\right] . \end{aligned} \tag{20}$$

Equation (19) should be applied at both $z = L/2$ and $z = -L/2$, with the dynamic magnetization given by Eq. (14) or (15). This leads to a 4×4 matrix equation for α, β, γ, and δ.

III. COMPUTATIONS

It is convenient to introduce dimensionless variables,

$$z' = 2z/L , \tag{21}$$

and so the film extends from $z' = -1$ to $z' = 1$. The wave vectors are also redefined,

$$k' = kL/2, \quad \mu' = \mu L/2, \quad \tau' = \tau L/2 , \tag{22}$$

and so are the pinning parameters,

$$p' = pL/2, \quad q' = qL/2, \quad r' = rL/2 . \tag{23}$$

From now on we omit the primes.

With given values for L, A, ω, g, and M, and assuming values for $(\partial_n M)/M$, the bulk anisotropy energy $E(\varphi,\vartheta)$, and the surface energy $F(\varphi,\vartheta)$, one obtains for any magnetic field H applied in the ϕ,θ directions the equilibrium angles φ,ϑ of the static magnetization $\mathbf{M}$ from Eqs. (5) and (6); values of P, Q, and R from Eq. (8); the wave vectors k (or μ) and τ from Eqs. (12) and (13); $e^{\pm}$ and $g^{\pm}$ functions from Eqs. (16) and (17); and the pinning parameters p, q, and r at both surfaces from Eq. (20). Then the boundary conditions (19) are of the form

$$\sum_{j=1}^{4} a_{ij} x_j = 0 , \tag{24}$$

where $x_1 = \alpha$, $x_2 = \beta$, $x_3 = \gamma$, $x_4 = \delta$, and

$$\begin{aligned} a_{11} &= (e^+ g^- p_2 + i e^- g^+ r_2)\sin k + e^+ g^- k\cos k , \\ a_{12} &= (e^+ g^- p_2 + i e^- g^+ r_2)\cos k - e^+ g^- k\sin k , \\ a_{13} &= (e^- g^- p_2 - i e^+ g^+ r_2)\exp(-\tau)\sinh\tau \\ &\quad + e^- g^- \tau\exp(-\tau)\cosh\tau , \\ a_{14} &= (e^- g^- p_2 - i e^+ g^+ r_2)\exp(-\tau)\cosh\tau \\ &\quad + e^- g^- \tau\exp(-\tau)\sinh\tau , \\ a_{21} &= (e^+ g^- p_1 + i e^- g^+ r_1)\sin k + e^+ g^- k\cos k , \\ a_{22} &= -(e^+ g^- p_1 + i e^- g^+ r_1)\cos k + e^+ g^- k\sin k , \\ a_{23} &= (e^- g^- p_1 - i e^+ g^+ r_1)\exp(-\tau)\sinh\tau \\ &\quad + e^- g^- \tau\exp(-\tau)\cosh\tau , \\ a_{24} &= -(e^- g^- p_1 - i e^+ g^+ r_1)\exp(-\tau)\cosh\tau \\ &\quad - e^- g^- \tau\exp(-\tau)\sinh\tau , \\ a_{31} &= (e^- g^+ q_2 - i e^+ g^- r_2)\sin k + e^- g^+ k\cos k , \\ a_{32} &= (e^- g^+ q_2 - i e^+ g^- r_2)\cos k - e^- g^+ k\sin k , \\ a_{33} &= -(e^+ g^+ q_2 + i e^- g^- r_2)\exp(-\tau)\sinh\tau \\ &\quad - e^+ g^+ \tau\exp(-\tau)\cosh\tau , \\ a_{34} &= -(e^+ g^+ q_2 + i e^- g^- r_2)\exp(-\tau)\cosh\tau \\ &\quad - e^+ g^+ \tau\exp(-\tau)\sinh\tau , \\ a_{41} &= (e^- g^+ q_1 - i e^+ g^- r_1)\sin k + e^- g^+ k\cos k , \\ a_{42} &= -(e^- g^+ q_1 - i e^+ g^- r_1)\cos k + e^- g^+ k\sin k , \\ a_{43} &= -(e^+ g^+ q_1 + i e^- g^- r_1)\exp(-\tau)\sinh\tau \\ &\quad - e^+ g^+ \tau\exp(-\tau)\cosh\tau , \\ a_{44} &= (e^+ g^+ q_1 + i e^- g^- r_1)\exp(-\tau)\cosh\tau \\ &\quad + e^+ g^+ \tau\exp(-\tau)\sinh\tau , \end{aligned} \tag{25}$$

for volume modes, $k^2 d > 0$. Index 1 refers to the lower plane $z = -1$ and index 2 is for the upper plane $z = 1$. For surface modes, $k^2 d < 0$, a formal substitution in Eq. (25) is

$$\begin{aligned} &\sin k \to \exp(-\mu)\sinh\mu , \\ &\cos k \to \exp(-\mu)\cosh\mu , \\ &k\sin k \to -\exp(-\mu)\mu\sinh\mu , \\ &k\cos k \to \exp(-\mu)\mu\cosh\mu . \end{aligned} \tag{26}$$

Equation (24) has nonzero solutions only if

$$\det(a_{ij}) = 0 . \tag{27}$$

By scanning the applied field H, one obtains the resonance fields H_n (and also k_n) for which Eq. (27) is satisfied. The nth solution for α, β, γ, and δ is then given except for an arbitrary multiplication factor. Thus the dynamic magnetization distribution $\mathbf{m}(z)$ given by Eqs. (14) and (15) may be used for calculations of the intensity I_n of the nth mode.[2-4,11,18] For the microwave driving field in the x-y film plane along the $\hat{\varphi}$ direction, which is a commonly used configuration of the magnetic fields in experiment, we have

$$I_n = \left[\int_{-1}^{1} dz\, m_\varphi/i\right]^2 \Big/ \int_{-1}^{1} dz\,[m_\vartheta^2 + (m_\varphi/i)^2] , \tag{28}$$

and the arbitrary multiplication factor is irrelevant in Eq.

(28). Normalization of the intensity is such that in perpendicular ferromagnetic resonance when $m_\vartheta = m_\varphi / i = \text{const}, I = 1$.

The above procedure is an exact one. In the SWM approximation one ignores the τ mode corresponding to the opposite polarization of $\mathbf{m}$. It is argued that this antiresonance mode is negligible since the imaginary wave vector with $\tau \gtrsim (\Omega L^2/4d)^{1/2}$ is usually a large number, and therefore this mode is heavily damped. The SWM approach is equivalent to setting $\gamma = \delta = 0$. Then all four boundary equations cannot be satisfied simultaneously. In the SWM one considers only the first condition in Eq. (19), $\partial_n m_\vartheta + p m_\vartheta + r m_\varphi = 0$, which produces just two equations for α and β.

In most cases the surface energy $F(\varphi,\vartheta)$ is assumed to be φ independent and then $r=0$. Also, one can always choose the coordinate system so that $R=0$. The determinant (27) is then for volume modes

$$\det(a_{ij}) = \{[1+2w^2-2w(1+w^2)^{1/2}]K(q_1,q_2,k)T(p_1,p_2,\tau)+[1+2w^2+2w(1+w^2)^{1/2}]K(p_1,p_2,k)T(q_1,q_2,\tau) + K(p_1,q_2,k)T(p_2,q_1,\tau)+K(p_2,q_1,k)T(p_1,q_2,\tau)-2(p_1-q_1)(p_2-q_2)k\tau\exp(-2\tau)\}\Omega^2 , \tag{29}$$

where

$$w = \Delta/\Omega = (P-Q)/2\Omega , \tag{30}$$

$$K(x,y,k) = (xy-k^2)\sin(2k)+(x+y)k\cos(2k) , \tag{31}$$

$$T(x,y,\tau) = [(xy+\tau^2)\sinh(2\tau)+(x+y)\tau\cosh(2\tau)]\exp(-2\tau) . \tag{32}$$

For surface modes, $0 < -k^2 d = \mu^2 d$,

$$\det(a_{ij}) = \{[1+2w^2-2w(1+w^2)^{1/2}]T(q_1,q_2,\mu)T(p_1,p_2,\tau)+[1+2w^2+2w(1+w^2)^{1/2}]T(p_1,p_2,\mu)T(q_1,q_2,\tau) + T(p_1,q_2,\mu)T(p_2,q_1,\tau)+T(p_2,q_1,\mu)T(p_1,q_2,\tau)-2(p_1-q_1)(p_2-q_2)\mu\tau\exp(-2\mu-2\tau)\}\Omega^2 . \tag{33}$$

IV. EXAMPLE: CASE OF UNIAXIAL ANISOTROPY

Here we assume the bulk anisotropy energy to be of the form $E(\varphi,\vartheta) = K\sin^2\vartheta$ and the usually postulated surface energy $F(\varphi,\vartheta) = K_s \sin^2\vartheta$. We can choose the static magnetic field to be applied in the x-z plane, $\phi = 0$, and then $\varphi = 0$. The equilibrium condition (5) now reads

$$u\sin(2\vartheta)+h\sin(\vartheta-\theta)=0 , \tag{34}$$

where

$$u = \left[\frac{2K}{4\pi M^2}-1\right]\Big/2, \quad h = H/4\pi M . \tag{35}$$

Currently we have $R=0$ and

$$\begin{aligned} P &= h\cos(\vartheta-\theta)+2u\cos^2\vartheta , \\ Q &= h\cos(\vartheta-\theta)+2u\cos(2\vartheta) , \\ \Delta &= u\sin^2\vartheta . \end{aligned} \tag{36}$$

The pinning parameters (20) are $r=0$ and

$$\begin{aligned} p &= \frac{L}{2}\left[\frac{K_s}{A}\cos(2\vartheta)-(\partial_n M)/M\right] , \\ q &= \frac{L}{2}\left[\frac{K_s}{A}\cos^2\vartheta-(\partial_n M)/M\right] . \end{aligned} \tag{37}$$

Let us discuss the perpendicular resonance first, $\theta=0$. In saturation, $h > -2u$, the static magnetization is along the z axis and $\vartheta = 0$. Then $p=q$ and the determinant (29) is greatly simplified. We obtain for the volume modes the well-known equation for allowed k vectors,

$$(p_1p_2-k^2)\sin 2k+(p_1+p_2)k\cos(2k)=0 . \tag{38}$$

The resonance field is given by

$$h = \Omega - 2u - \frac{4d}{L^2}k^2 , \tag{39}$$

and the intensity

$$I = \frac{2\beta^2\sin^2(k)/k^2}{\alpha^2[1-\sin(2k)/2k]+\beta^2[1+\sin(2k)/2k]} . \tag{40}$$

For surface modes

$$(p_1p_2+\mu^2)\sinh(2\mu)+(p_1+p_2)\mu\cosh(2\mu)=0 , \tag{41}$$

$$h = \Omega - 2u + \frac{4d}{L^2}\mu^2 , \tag{42}$$

$$I = \frac{2\beta^2\sinh^2(\mu)/\mu^2}{\alpha^2[-1+\sinh(2\mu)/2\mu]+\beta^2[1+\sinh(2\mu)/2\mu]} . \tag{43}$$

The τ modes are obtained by replacing $\mu \to \tau$ and $\Omega \to -\Omega$. For k and μ modes $m_\vartheta = m_\varphi / i$; for the τ mode $m_\vartheta = -m_\phi / i$.

It is customary to discuss the phase diagram on the (p_1,p_2) plane and the modes labeling for the perpendicular resonance. There are three regions: I, II, and III (see Fig. 1), separated by critical curve

$$\frac{1}{p_1}+\frac{1}{p_2} = -2 . \tag{44}$$

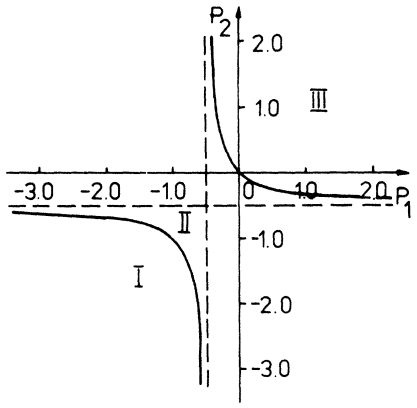

FIG. 1. The critical curve $1/p_1+1/p_2=-2$ for perpendicular resonance. Two surface modes are present in region I, one surface mode appears in region II, and only volume modes are allowed in region III.

In region I we have (i) mode $n=1$, surface mode with $\mu>(|p_1p_2|)^{1/2}$ and

$$\alpha=-(\mu\sinh\mu+p_2\cosh\mu)=\mu\sinh\mu+p_1\cosh\mu\ , \tag{45}$$

$$\beta=\mu\cosh\mu+p_2\sinh\mu=\mu\cosh\mu+p_1\sinh\mu\ ;$$

(ii) mode $n=2$, surface mode with $\mu<(|p_1p_2|)^{1/2}$ and the same α,β as for mode 1; (iii) modes $n=3,4,5,\ldots$, volume modes with $(n-2)\pi/2<k<(n-1)\pi/2$ and

$$\alpha=k\sin k-p_2\cos k=-k\sin k+p_1\cos k\ , \tag{46}$$

$$\beta=k\cos k+p_2\sin k=k\cos k+p_1\sin k\ .$$

In region II there appears (i) mode $n=1$, surface mode, as in region I; (ii) mode $n=2$, volume mode with $0<k<3\pi/4$ and α,β given by Eq. (46); (iii) modes $n=3,4,5,\ldots$, volume modes with $(2n-3)\pi/4<k<(2n-1)\pi/4$ and α,β given by Eq. (46).

In region III there are only volume modes: modes $n=1,2,3,\ldots$, volume modes with $(n-1)\pi/2<k<n\pi/2$ and α,β given by Eq. (46).

Some analytical results are summarized in Table I for symmetrical pinning $p_1=p$ and $p_2=p$. Table II gives results for the nonsymmetrical case $p_1=p$ and $p_2=0$. The antisymmetrical case $p_1=p$ and $p_2=-p$ is shown in Table III. In perpendicular resonance both SWM and the circular-precession-approximation calculations give rigorous results. Mode labeling is easy, at least in the saturation region when an increasing mode number corresponds to a decreasing resonance field. In experiments some care is necessary to prevent us from skipping over the modes with zero intensities, see Tables I and III.

For nonperpendicular resonance $\theta\neq0$. Then the circular precession, SWM, and the exact results differ from each other. For symmetrical boundary conditions the even modes vanish since $\beta=\delta=0$, and so the magnetization m is antisymmetrical in z. For asymmetrical-pinning conditions all modes are present. The antisymmetrical boundary conditions yield zero intensity for odd modes only in perpendicular resonance; in the SWM approximation the odd modes vanish for any angle θ.

V. RESULTS OF CALCULATIONS

Calculations were carried out for a set of parameters typical for a Permalloy polycrystalline thin film: $L=1000$ Å, $A=0.5\times10^{-6}$ erg/cm, microwave frequency $f=9.6$ GHz, and $M=800$ G. We assumed the g factor $g=2$ and no variation of the magnetization in the presurface layer, $(\partial_nM)/M=0$. Results for some values of the pinning parameters are collected in Tables IV, V, and VI. Numbers resulting from the exact calculations are followed by numbers of the SWM model. As was mentioned before, for $\theta=0$ the two models are identical. In the wave-vector column, positive values are k's, indicating the volume solution, negative ones are μ's for surface modes.

Table IV contains three examples of strong negative, weak, and strong positive symmetrical pinnings. Even modes are not shown since their intensities $I=0$. Perhaps it is illustrative to discuss in more detail the mode labeling, say for the case of strong negative pinning. For $\theta=0$ we obtain resonance fields, in descending order, for modes $n=1$, 2, 3, 4, 5, and 6 for saturated fields when $\vartheta=0$; then we label modes as 6′, 5′, and 4′ for nonsaturated

TABLE I. Perpendicular resonance with symmetrical boundary conditions $p_1=p$ and $p_2=p$.

Mode	Allowed wave vectors	α	β	Intensity	Remarks
$n=1,\ p<0$	$p=-\mu\tanh\mu$	0	1	$\frac{2\sinh^2(\mu)/\mu^2}{1+\sinh(2\mu)/2\mu}$	$\mu>\lvert p\rvert$
$n=1,\ p>0$	$p=k\tan k$	0	1	$\frac{2\sin^2(k)/k^2}{1+\sin(2k)/2k}$	$0<k<\pi/2$
$n=2,\ p<-1$	$p=-\mu\coth\mu$	1	0	0	$\mu<\lvert p\rvert$
$n=2,\ p>-1$	$p=-k\cot k$	1	0	0	$0<k<\pi$
$n=3,5,7,\ldots$	$p=k\tan k$	0	1	$\frac{2\sin^2(k)/k^2}{1+\sin(2k)/2k}$	$(n-2)\pi/2<k<n\pi/2$
$n=4,6,8\ldots$	$p=-k\cot k$	1	0	0	$(n-2)\pi/2<k<n\pi/2$

TABLE II. Perpendicular resonance with nonsymmetrical boundary conditions $p_1=p$ and $p_2=0$.

Mode	Allowed wave vectors	α	β	Intensity	Remarks
$n=1,\ p<0$	$p=-\mu\tanh(2\mu)$	$-\tanh\mu$	1	$\frac{4}{(4\mu)^2}\frac{\cosh(4\mu)-1}{\sinh(4\mu)/4\mu+1}$	$\mu>\lvert p\rvert$
$n=1,\ p>0$	$p=k\tan(2k)$	$\tan k$	1	$\frac{4}{(4k)^2}\frac{1-\cos(4k)}{\sin(4k)/4k+1}$	$0<k<\pi/4$
$n=2,3,4,\ldots$	$p=k\tan(2k)$	$\tan k$	1	$\frac{4}{(4k)^2}\frac{1-\cos(4k)}{\sin(4k)/4k+1}$	$(2n-3)\pi/4<k<(2n-1)\pi/4$

TABLE III. Perpendicular resonance with antisymmetrical boundary conditions $p_1=p$ and $p_2=-p$.

Mode	Allowed wave vectors	α	β	Intensity
$n=1$	$\mu=\lvert p\rvert$	1	1	$\tanh(\mu)/\mu$
$n=2,4,6,\ldots$	$k=(n-1)\pi/2$	k	$-p$	$2p^2/[k^2(k^2+p^2)]$
$n=3,5,7,\ldots$	$k=(n-1)\pi/2$	p	k	0

TABLE IV. Spin-wave spectra for symmetrical boundary conditions $K_{s1}L/2A=K_{s2}L/2A=\tilde{p}$. The angle θ is in degrees. Numbers in the first column result from present calculations, numbers in the second column are obtained from the single-wave-vector model. The two models are identical for $\theta=0$. Positive wave vectors are k's, negative ones are μ's.

			H_n (Oe)		I_n		k or μ	
$\tilde{p}$	θ	n	1	2	1	2	1	2
−5.0	0	1	14733		0.400		−5.00	
		3	13294		0.558		1.94	
		5	11942		0.032		5.55	
	10	1	7565	6480	1.044	0.966	−1.70	1.06
		3	3819	1551	0.002	0.065	3.06	4.01
	90	1	1043	972	1.292	0.913	0.55	1.31
		3	532	245	0.003	0.066	3.24	4.03
0.2	0	1	13473		0.999		0.43	
		3	12969		0.001		3.20	
		5	11489		0.000		6.31	
	10	1	6787	6818	1.012	1.000	0.22	−0.26
		3	3643	3751	0.000	0.001	3.14	3.09
	90	1	1059	1069	1.018	0.999	−0.13	−0.46
		3	567	585	0.000	0.001	3.14	3.08
5.0	0	1	13396		0.913		1.31	
		3	12669		0.066		4.03	
		5	11095		0.013		6.91	
	10	1	6590	7303	1.180	0.947	0.86	−1.36
		3	3681	5267	0.000	0.310	3.13	2.24
	90	1	1097	2307	1.283	0.400	−0.87	−5.00
		3	628	870	0.017	0.558	2.93	1.94

TABLE V. Spin-wave spectra for asymmetrical boundary conditions $K_{s_1}L/2A=0$ and $K_{s_2}L/2A=\tilde{p}$. See Table IV for description.

			H_n (Oe)		I_n		k or μ	
$\tilde{p}$	θ	n	1	2	1	2	1	2
−5.0	0	1	14733		0.200		−5.00	
		2	13445		0.707		0.87	
		3	13146		0.063		2.60	
		4	12556		0.017		4.28	
		5	11722		0.006		5.93	
		6	10623		0.003		7.56	
	10	1	7439	6694	0.730	0.936	−1.55	0.61
		2	6391	5570	0.243	0.068	1.19	2.02
		3	3723	2631	0.000	0.021	3.11	3.58
	90	1	1052	1033	1.199	0.874	0.37	0.71
		2	919	827	0.009	0.084	1.67	2.15
		3	584	405	0.001	0.023	3.19	3.61
5.0	0	1	13457		0.874		0.71	
		2	13251		0.084		2.15	
		3	12829		0.024		3.61	
		4	12182		0.009		5.10	
		5	11300		0.004		6.61	
		6	10178		0.002		8.13	
	10	1	6716	7237	1.067	0.732	0.55	−1.27
		2	5881	6490	0.025	0.443	1.76	1.04
		3	3665	4528	0.000	0.045	3.13	2.70
	90	1	1083	2308	1.210	0.200	−0.70	−5.00
		2	966	1020	0.076	0.707	1.36	0.87
		3	596	722	0.003	0.063	3.04	2.60

fields when $\vartheta \neq 0$. Obviously, this single-domain model may fail, especially for the perpendicular case and a nonsaturated sample, when many-domains structure may develop. For this reason the 6′, 5′, and 4′ modes are not included in Table IV. However, if we assume the single-domain model is still valid, the labeling follows from the fact that the wave vectors of modes 6 and 6′ are close to each other, and also those of the 5,5′ and 4,4′ modes. It seems more justified to label the modes according to the peak position in k space rather than in descending magnetic-field order. In experiments only odd modes 1, 3, 5, and 5′ are visible. Of course, moving off the $p_1=p_2$ line we obtain, although small at first, nonzero intensities of the other modes also. This is the situation for $\theta=0$. With increasing θ, the separation of resonance fields of modes 6 and 6′ tends to zero and the two modes disappear at a critical angle θ_0. The two modes correspond to two adjacent zeros of the determinant (29) as a function of the applied field H. Above the critical angle θ_0, $\det(a_{ij})$ has no solution as the local maximum goes down so that $\det(a_{ij})$. Further increase in θ makes modes 5 and 5′ disappear, then modes 4 and 4′ also vanish. Finally, only modes 1, 2, and 3 survive for θ greater than about 5°. The case of weak pinning provides the same sequence of modes. In the case of strong positive pinning we have $n=1$, 2, 3, 4, 5, and 5′ modes for $\theta=0$. The first four are still present for parallel resonance.

Table V shows the results for asymmetrical boundary conditions when one surface is unpinned $p_2=0$, and spins at the other surface are strongly pinned. In this case all modes have nonzero intensities. As in the symmetrical case we have modes $n=1$, 2, 3, 4, 5, 6, 6′, 5′, and 4′ for perpendicular resonance. With increasing θ, the 6,6′ pair vanishes first, then the 5,5′ pair, followed by disappearance of the 4,4′ pair of modes.

For antisymmetrical boundary conditions the results are collected in Table VI. Odd modes $n=3,5,7,\ldots$ have zero intensities for the SWM model. The exact calculations yield small $I\neq 0$ except for the perpendicular resonance when $I=0$. The sequence of the critical angles θ_0 are same as in the symmetrical case.

There is another possible mechanism of approaching a critical angle θ_c (or ϑ_c) at which intensity $I=0$. This happens when the integral of $m(z)$ as a function of the angle θ changes its sign. Now, unlike the previous case, the mode still exists for $\theta>\theta_c$. This is the situation, for example, for mode $n=3$ of strong positive symmetrical pinning, Table IV, when $\theta_c\approx 10°$, which corresponds to $\vartheta_c\approx 70°$; or mode $n=2$ of antisymmetrical pinning, Table VI, with $\theta_c\approx 15°$ and $\vartheta_c\approx 70°$.

TABLE VI. Spin-wave spectra for antisymmetrical boundary conditions $K_{s1}L/2A = -K_{s2}L/2A = 5$. See Table IV for description.

		H_n (Oe)		I_n		k or μ	
θ	n	1	2	1	2	1	2
0	1	14733		0.200		−5.00	
	2	13359		0.738		1.57	
	4	12372		0.048		4.71	
	6	10398		0.009		7.85	
10	1	7432	7230	0.692	0.676	−1.54	−1.26
	2	6127	6077	0.281	0.536	1.52	1.57
	3	3736	3646	0.001	0	3.10	3.14
15	1	4309	5718	1.171	0.357	−0.42	−2.78
	2	3841	3788	0.002	0.698	1.48	1.57
	3	2339	2282	0.001	0	3.10	3.14
90	1	1079	2308	1.162	0.200	−0.64	−5.00
	2	948	935	0.123	0.738	1.49	1.57
	3	579	565	0.001	0	3.10	3.14

VI. DISCUSSION

General boundary condition (19) produces a set of four equations, and so the test functions for the microwave magnetization must be a superposition of four wavelike solutions. If, as it is usually assumed, the surface energy is φ independent, then $r=0$ in Eq. (20). If also $p=q$, the two pairs of equations (19) are identical and so a single k mode, $\alpha\sin(kz)+\beta\cos(kz)$, is a proper test function corresponding to the SWM model. In general, however, $p\neq q$ due to the different angular dependence of the surface anisotropy terms. Therefore it is only for perpendicular resonance or for no surface anisotropy, $F=0$, that the SWM model is correct. There is also an isotropic contribution to the pinning $(\partial_n M)/M$ due to the variation of magnetization near the surface. The isotropic and anisotropic parts of the pinning are compatible with parameters introduced in Puszkarski's theory.[5,19,20] His pinning parameter a can be expressed by our dimensionless pinning p; the relation is $a=1-2p/S$, where S is number of atomic layers along the normal to the film plane.

Detailed comparison of the model with experiment is difficult. We still lack a well-established theory that would predict simultaneously all mode positions and their intensities in satisfactory agreement with observed values even for perpendicular resonance. The presented approach which falls into the SWM model for the perpendicular resonance obviously cannot provide any better agreement for this configuration. Assumed uniform magnetization, no eddy-current contribution, and many other factors may be thought of as responsible for only qualitative agreement between theory and experiment. We still hope that the presented model may bring in some new features for the nonperpendicular configuration.

For example, the usually claimed to be expected value of the critical angle ϑ_c is 45°. In the SWM model when Eqs. (38) and (40) still hold for any angle ϑ, $I=0$ requires that $k=n\pi$, and therefore $p_1+p_2=0$ according to Eq. (38). With no variation of the static magnetization in the presurface region, $\partial_n M=0$, we obtain from Eq. (37) $p\sim\cos 2\vartheta$, and so $\vartheta_c=45°$. However, the observed values of ϑ_c (Refs. 21–23) are different from 45°. It was then concluded[23] that $\partial_n M\neq 0$. Such a conclusion is not fully justified since the exact calculations indicate that $\vartheta_c\neq 45°$ even if $\partial_n M=0$.

It also should be noted that the $p_1+p_2=0$ condition always predicts a k-independent value. However, there is firm experimental evidence[21,22] that ϑ_c decreases with increasing k. This also results from our exact calculations. The angular dependence of ϑ_c was also obtained by Jirsa[13–15] from his model based on a similar two-wave-mode assumption.

The rigorous model predicts the presence of odd modes for antisymmetrical pinning while these modes were prohibited in the SWM approximation (for a uniform driving rf field). The same was also found in Ref. 14.

Two different types of critical angles are expected: the angle θ_0 above which a pair of modes cease to exist and angle θ_c at which the intensity is zero, yet for $\theta>\theta_c$ the mode is still present. The latter takes place when the integral of $m(z)$ changes its sign with increasing θ. Then we expect $I\sim(\theta-\theta_c)^2$ near the critical angle θ_c. This can be seen, for example, for modes 6, 8, and 10 shown in Fig. 1 of Ref. 22. Different behavior is expected near θ_0. The intensities of the two adjacent modes should be equal when approaching θ_0 and not necessarily as $I\to 0$. Also, a rapid change ΔH in the separation of the resonance fields between the two modes is predicted, $\Delta H\sim(\theta_0-\theta)^{1/2}$. This requires a very fine experiment with large angular resolution. Also, the two modes nearly overlap before they disappear. For these reasons it may be difficult to trace experimentally the region of θ close to θ_0. Yet, it is a well-known fact that higher-order modes vanish with increasing θ. In more recent papers[24,25] the authors observed as many as 11 lines for $\theta=0$ in a single-crystal nickel film. With increasing θ higher-order modes disappeared. Modes 11 and 10 vanished, then the 9 and 8 pair was missed, and at $\theta=5°$ only the first 7 lines were visible. Further increase in θ made the 7 and 6 pair vanish, and, finally, only two lines were left for the parallel resonance.

In these calculations we ignored the $(\partial_n M)/M$ contribution to the pinning parameters for simplicity. However, rough estimation indicates that this term may be significant and should be, as rule, included. Also, the commonly postulated surface-energy term $K_s \sin^2\vartheta$ does not reflect the symmetry at the surface for monocrystalline samples and perhaps higher-order φ-dependent terms[19] as $\cos 2\varphi$ or $\cos 4\varphi$ should be accounted for in $F(\varphi,\vartheta)$. A more realistic model must also take into account imperfections and conduction in the samples.

ACKNOWLEDGMENTS

The author thanks Professor H. Puszkarski for useful discussions. This work was partially supported by the Polish Academy of Sciences.

[1]A. M. Portis, Appl. Phys. Lett. **2**, 69 (1963).
[2]F. Hoffmann, Solid State Commun. **9**, 295 (1971).
[3]L. J. Maksymowicz, A. Z. Maksymowicz, and K. D. Leaver, Solid State Commun. **18**, 1413 (1976).
[4]M. Sparks, Phys. Rev. B **1**, 3869 (1970).
[5]H. Puszkarski, Acta Phys. Pol. A **38**, 217 (1970); **38**, 899 (1970).
[6]J. Spałek and A. Z. Maksymowicz, Solid State Commun. **15**, 559 (1974).
[7]H. Puszkarski, Phys. Status Solidi B **96**, 61 (1979).
[8]C. Vittoria, R. C. Barker, and A. Yelon, J. Appl. Phys. **40**, 1561 (1969).
[9]I. Harada, O. Nagai, and T. Nagamiya, Phys. Rev. B **16**, 4882 (1977).
[10]Diep-The-Hung and J. C. Lèvy, Surf. Sci. **80**, 512 (1979).
[11]M. Sparks, Phys. Rev. B **1**, 3831 (1970).
[12]J. Spałek, Phys. Status Solidi B **64**, K9 (1974).
[13]M. Jirsa, Phys. Status Solidi B **124**, 609 (1984).
[14]M. Jirsa, Phys. Status Solidi B **125**, 187 (1984).
[15]M. Jirsa and V. Kambersky, Phys. Status Solidi B **126**, 547 (1984).
[16]G. T. Rado and J. R. Weertman, J. Phys. Chem. Solids **11**, 315 (1959).
[17]P. Pincus, Phys. Rev. **118**, 658 (1960).
[18]A. Z. Maksymowicz, Thin Solid Films **42**, 245 (1977).
[19]A. P. Cracknell and H. Puszkarski, Solid State Commun. **28**, 891 (1978).
[20]H. Puszkarski, Prog. Surf. Sci. **9**, 191 (1979).
[21]M. Okochi and H. Nose, J. Phys. Soc. Jpn. **27**, 312 (1969).
[22]F. Hoffmann, Phys. Rev. B **4**, 1604 (1971).
[23]L. J. Maksymowicz and D. Sendorek, J. Magn. Magn. Mater. **37**, 177 (1983).
[24]D. P. Mitra and J. S. S. Whiting, J. Phys. F **8**, 2401 (1978).
[25]J. S. S. Whiting, IEEE Trans. Magn. **MAG-18**, 709 (1982).